*Inorg. Chem.* **2006**, *45*, 2886–2895


# Controlling Aggregation of Copper(II)-Based Coordination Compounds: From Mononuclear to Dinuclear, Tetranuclear, and Polymeric Copper Complexes

**John Fielden,[†] Joanna Sprott,[†] De-Liang Long,[†] Paul Kögerler,[‡] and Leroy Cronin*,[†]**

*Department of Chemistry, Joseph Black Building, University of Glasgow, University Avenue, Glasgow, G12 8QQ, United Kingdom, and Ames Laboratory, Iowa State University, Ames, Iowa 50011*

Received September 24, 2005

The use of a strategy combining ligand design and changes of reaction conditions has been investigated with the goal of directing the assembly of mononuclear, dinuclear, tetranuclear, and polymeric copper(II) complexes. As a result, closely related copper monomers, alkoxo dimers, and hydroxo cubanes, along with a carbonate-bridged polymeric species, have been synthesized using the rigid, aliphatic amino ligands *cis*-3,5-diamino-*trans*-hydroxycyclohexane (DAHC), *cis*-3,5-diamino-*trans*-methoxycyclohexane (DAMC), and the glutaryl-linked derivative glutaric acid bis-(*cis*-3,5-diaminocyclohexyl) ester (GADACE). The composition of the monomeric complex has been determined by X-ray crystallography as $[Cu(DAHC)_2](ClO_4)_2$ (**1**), the two dimers as $[\{Cu(DAHC)(OMe)\}_2](ClO_4)_2 \cdot MeOH$ (**2**) and $[\{Cu(DAMC)(OMe)(ClO_4)\}_2]$ (**3**), the three $Cu_4O_4$ cubanes as $[\{Cu(DAHC)(OH)\}_4](ClO_4)_4 \cdot 2.5MeOH$ (**4**), $[\{Cu(DAMC)(OH)\}_4](ClO_4)_4 \cdot H_2O$ (**5**), and $[\{Cu_2(OH)_2(GADACE)\}_2]Cl_4 \cdot 2MeOH \cdot 6H_2O$ (**6**), and an infinite-chain structure as $[\{Cu(DAHC)(CO_3)\}_n]$ (**7**). Furthermore, the cubane structures **4** and **5** have been investigated magnetically. Our studies indicate that formation of the monomeric, dimeric, and tetranuclear DAHC and DAMC complexes can be controlled by small changes in reaction conditions and that further preorganization of the ligand moiety by linking the DAHC cores (GADACE) allows more effective direction of the self-assembly of the $Cu_4O_4$ cubane core.

## Introduction

The controlled aggregation of small coordination-complex-based building blocks to form larger architectures is of great interest in both metal−ligand and polyoxometalate chemistry. In particular, the ability to use both ligand design and adjustment of reaction conditions to understand and control the aggregation processes is vital, since the combination of these approaches should give the best chance of designing and synthesizing sophisticated, potentially functional, complexes and clusters.[1−4]

A great motivation for progress in this area is the properties of a wide variety of multinuclear coordination compounds, both designed and "discovered", which have exhibited phenomena including single-molecule magnetism,[5,6] catalysis of organic reactions,[7,8] and, in many cases, structural and chemical similarity to active sites in metalloenzymes.[8−10] In this way, the study of polynuclear coordination compounds provides opportunities to cross boundaries between different areas of chemistry and also to interface with physics and biology.

* To whom correspondence should be addressed. E-mail: L.Cronin@chem.gla.ac.uk.
[†] University of Glasgow.
[‡] Iowa State University.

(1) Hegetschweiler, K.; Morgenstern, B.; Zubieta, J.; Hagrman, P. J.; Lima, N.; Sessoli, R.; Totti, F. *Angew. Chem., Int. Ed.* **2004**, *43*, 3436.
(2) Morgenstern, B.; Steinhauser, S.; Hegetschweiler, K.; Garribba, E.; Micera, G.; Sanna, D.; Nagy, L. *Inorg. Chem.* **2004**, *43*, 3116.
(3) Applegarth, L.; Goeta, A. E.; Steed, J. W. *Chem. Commun.* **2005**, 2405.
(4) Turner, D. R.; Hursthouse, M. B.; Light, M. E.; Steed, J. W. *Chem. Commun.* **2004**, 1354.
(5) Cadiou, C.; Murrie, M.; Parsons, S.; Rawson, J. M.; Winpenny, R. E. P. *Chem. Commun.* **2001**, 2666.
(6) Gatteschi, D.; Sessoli, R. *J. Magn. Magn. Mater.* **2004**, *272−276*, 1030.
(7) Yoshizawa, M.; Takeyama, Y.; Kusukawa, T.; Fujita, M. *Angew. Chem., Int. Ed.* **2002**, *41*, 1347.
(8) Ackermann, J.; Meyer, F.; Kaifer, E.; Pritzkow, H. *Chem.—Eur. J.* **2002**, *8*, 247.
(9) Beinert, H.; Holm, R. H.; Münck, E. *Science* **1997**, *277*, 653.
(10) Johnson, M. K.; Duderstadt, R. E.; Duin, E. C. *Adv. Inorg. Chem.* **1999**, *47*, 1.



10.1021/ic051647t CCC: $33.50 
Published on Web 03/07/2006

While rational design strategies have enjoyed considerable success in controlling the structure of such compounds by employing large, rigid ligands and metal centers with well-defined coordination preferences,[11,12] the results of using smaller ligands and metals offering multiple coordination modes (e.g., copper(II)) are less predictable.[13,14] In this case, the directing and templating effects of the ligands are weaker, and other variables, most notably the coordination or hydrogen bonding abilities of the solvent or counterion, can cause changes as significant as a different cluster nuclearity[15] or as subtle as different crystal packing.[16] We hope that careful consideration of the types of cluster formed in different conditions might increase the understanding of these systems and eventually allow a more rational approach in this field.

Progress in understanding this type of self-assembly process is likely to be developed by first studying relatively small, simple aggregates. We were recently able to describe an unusual solvent-controlled reversible geometry reorganization in a mononuclear copper(II) fluoride complex of *cis*-3,5-diamino-*trans*-hydroxycyclohexane (DAHC),[17] a small, rigid ligand capable of acting as a chelator in its bis-axial conformation. The solvent control appears to be the result of a fine balance between the stability of the hydrogen bonded network and the coordination preferences of the Cu(II) center.[17] In this study, we have extended this work to investigate the polynuclear copper(II) coordination chemistry of DAHC, its methyl derivative *cis*-3,5-diamino-*trans*-methoxycyclohexane (DAMC), and the tetradentate glutaric acid bis-(*cis*-3,5-diaminocyclohexyl) ester (GADACE), which connects two DAHC chelating units through a glutaryl ester linkage. Particular attention has been paid to the influence of solvent and pH on the classes of compounds formed and how this influence might be exerted. Of these compound types the copper−oxo dimers and cubanes are particularly well studied in coordination chemistry[8,18] and biology[19−22] because of their magnetic properties[23−28] and similarity to the active site of the enzyme catechol oxidase.[8,18,29] To complement the focus on the structures and conditions for their formation, the magnetic properties of the $Cu_4O_4$ cubanes have been investigated and seven new architectures are presented that span diverse architectures from monomeric units, $[Cu(DAHC)_2](ClO_4)_2$ (**1**), to dimers, $[\{Cu(DAHC)(OMe)\}_2](ClO_4)_2 \cdot MeOH$ (**2**) and $[\{Cu(DAMC)(OMe)(ClO_4)\}_2]$ (**3**), to tetramers, $[\{Cu(DAHC)(OH)\}_4](ClO_4)_4 \cdot 2.5MeOH$ (**4**), $[\{Cu(DAMC)(OH)\}_4](ClO_4)_4 \cdot H_2O$ (**5**), and $[\{Cu_2(OH)_2(GADACE)\}_2]Cl_4 \cdot 2MeOH \cdot 6H_2O$ (**6**), and to the infinite-chain structure $[\{Cu(DAHC)(CO_3)\}_n]$ (**7**).

## Experimental Section

**Materials, Methods, and Instrumentation.** The ligands *cis*-3,5-diamino-*trans*-hydroxycyclohexane (DAHC), *cis*-3,5-diamino-*trans*-methoxycyclohexane (DAMC), and glutaric acid bis-(*cis*-3,5-diaminocyclohexyl) ester (GADACE) were synthesized starting from *cis*-1,3,5-cyclohexanetriol.[30] All other reagents and solvents were bought commercially as AR grade (Aldrich/Lancaster) and used without further purification. Complexations were performed in the ambient atmosphere, using between 0.52 and 0.7 mol of copper(II) salt/mol of ligand chelating group. Larger amounts of metal resulted in rapid precipitation of unidentified amorphous products. Infrared spectra were measured with Jasco FTIR-410 and Bruker TENSOR 27 spectrometers, and X-ray diffraction data were collected using a Nonius Kappa-CCD diffractometer with Mo Kα radiation and a graphite monochromator. Magnetic measurements were performed in the range of 2−290 K with a Quantum Design MPMS-5 SQUID magnetometer for a range of fields from 0.1 to 5.0 T.

**Preparation of $[Cu(DAHC)_2](ClO_4)_2$ (1) and $[\{Cu(DAHC)(CO_3)\}_n]$ (7).** Aqueous $NaClO_4$ ( 2 M, 0.25 mL) was added to a solution of DAHC (0.0704 g, 0.541 mmol) in methanol (20 mL), lowering the pH to ∼9.6. The addition of $Cu(ClO_4)_2 \cdot 6H_2O$ (0.1045 g, 0.282 mmol) in ca. 5 mL of methanol resulted in a deep purple solution of pH ∼7.3, which was stirred for 1 h before **1** was recovered as a red precipitate (0.0224 g, 0.0428 mmol, 15%). Reduction of the volume to 7.5 mL in vacuo, followed by removal of further precipitate and crystallization by evaporation and ether diffusion, yielded an inseparable mixture (0.028 g) of red crystals of **1**, dark blue crystals of $[\{Cu(DAHC)(OMe)\}_2](ClO_4)_2 \cdot MeOH$ (**2**), and a few light blue crystals of $[\{Cu(DAHC)(CO_3)\}_n]$ (**7**). Analytical data for **1**. IR (KBr disk, $cm^{-1}$): 3543 s, 3424 w, 3290 s, 3235 s, 2945 w, 2920 w, 2870 w, 1583 m, 1459 w, 1367 m, 1330 w, 1178 m, 1093 vs, 922 m, 688 w. Elemental analysis for $C_{12}H_{28}Cl_2CuN_4O_{10}$, actual (expected): C, 27.41 (27.57); H, 5.40 (5.40); N, 10.57 (10.72).

**Preparation of $[\{Cu(DAHC)(OMe)\}_2](ClO_4)_2 \cdot MeOH$ (2).** A methanolic solution (5 mL) of $Cu(ClO_4)_2 \cdot 6H_2O$ (0.1040 g, 0.280 mmol) was added to a solution of DAHC (0.0703 g, 0.539 mmol) in methanol (20 mL). A color change from the light blue of the copper(II) perchlorate to a clear deep blue was observed. After the mixture was stirred for 2.5 h, the volume was reduced to ca. 5 mL, at which point dark purple-black crystals started to form. After


(11) Fujita, M.; Umemoto, K.; Yoshizawa, M.; Fujita, N.; Kusukawa, T.; Biradha, K. *Chem. Commun.* **2001**, 509.
(12) Seidel, S. R.; Stang, P. J. *Acc. Chem. Res.* **2002**, *35*, 972.
(13) Winpenny, R. E. P. *Dalton Trans.* **2001**, 1.
(14) Matthews, C. J.; Avery, K.; Xu, Z. Q.; Thompson, L. K.; Zhao, L.; Miller, D. O.; Biradha, K.; Poirier, K.; Zaworotko, M. J.; Wilson, C.; Goeta, A. E.; Howard, J. A. K. *Inorg. Chem.* **1999**, *38*, 5266.
(15) Blake, A. J.; Brechin, E. K.; Codron, A.; Gould, R. O.; Grant, C. M.; Parsons, S.; Rawson, J. M.; Winpenny, R. E. P. *J. Chem. Soc., Chem. Commun.* **1995**, 1983.
(16) Murugesu, M.; Anson, C. E.; Powell, A. K. *Chem. Commun.* **2002**, 1054.
(17) Fielden, J.; Long, D.-L.; Cronin, L. *Chem. Commun.* **2004**, 2156.
(18) Than, R.; Feldmann, A. A.; Krebs, B. *Coord. Chem. Rev.* **1999**, *182*, 211.
(19) Klabunde, T.; Eicken, C.; Sacchettini, J. C.; Krebs, B. *Nature Struct. Biol.* **1998**, *5*, 1084.
(20) Kitajima, N.; Moro-oka, Y. *Chem. Rev.* **1994**, *94*, 737.
(21) Gerdemann, C.; Eicken, C.; Krebs, B. *Acc. Chem. Res.* **2002**, *35*, 183.
(22) Solomon, E. I.; Sundaram, U. M.; Machonkin, T. E. *Chem. Rev.* **1996**, *96*, 2563.
(23) Crawford, V. H.; Richardson, H. W.; Wasson, J. R.; Hodgson, D. J.; Hatfield, W. E. *Inorg. Chem.* **1976**, *15*, 2107.
(24) Ruiz, E.; Alemany, P.; Alvarez, S.; Cano, J. *Inorg. Chem.* **1997**, *36*, 3683.
(25) Ruiz, E.; Alemany, P.; Alvarez, S.; Cano, J. *J. Am. Chem. Soc.* **1997**, *119*, 1297.
(26) Hu, H. Q.; Zhang, D. J.; Chen, Z. D.; Liu, C. B. *Chem. Phys. Lett.* **2000**, *329*, 255.
(27) Ruiz, E.; Rodriguez-Fortea, A.; Alemany, P.; Alvarez, S. *Polyhedron* **2001**, *20*, 1323.
(28) Rodriguez-Fortea, A.; Ruiz, E.; Alvarez, S.; Alemany, P. *Dalton Trans.* **2005**, 2624.
(29) Zippel, F.; Ahlers, F.; Werner, R.; Haase, W.; Nolting, H. F.; Krebs, B. *Inorg. Chem.* **1996**, *35*, 3409.
(30) Fielden, J.; Sprott, J.; Cronin, L. *New J. Chem* **2005**, 1152.

filtration, the clear gray-blue solution was set to crystallize using evaporation or $Et_2O$ diffusion techniques. In each case, small dark purple-black cubic crystals of compound **2** (0.0497 g, 0.073 mmol, 52 %) were formed overnight. Upon isolation and exposure to air, they rapidly changed color becoming a royal blue hydroxo compound with the composition $C_{12}H_{30}Cl_2Cu_2N_4O_{12}$. IR (crystal in mother liquor, diamond anvil, $cm^{-1}$): 3272 s, 2945 m, 2833 m, 1450 w, 1411 w, 1106 w, 1023 vs, 804 w. IR (hydroxo compound, KBr disk, $cm^{-1}$): 3411 s, 3225 s, 3168 s, 3112 s, 2925 m, 2890 m, 2850 w, 1602 s, 1457 m, 1403 m, 1366 m, 1343 w, 1258 w, 1147 s, 1088s, 1057s, 1068 s, 913 m, 714 m, 627 s, 466 m, 404 w. Elemental analysis for $C_{12}H_{30}Cl_2Cu_2N_4O_{12}$, actual (expected): C, 23.25 (23.23); H, 4.84 (4.87); N, 8.77 (9.03).

**Preparation of [{Cu(DAMC)(OMe)($ClO_4$)}$_2$] (3).** To a solution of DAMC (0.050 g, 0.35 mmol) in methanol (20 mL) was added a methanolic solution (5 mL) of $Cu(ClO_4)_2 \cdot 6H_2O$ (0.091 g, 0.245 mmol). A color change from the light blue of the copper(II) perchlorate to a clear dark blue was observed. After the mixture was stirred for 30 min, the volume was reduced to ca. 15 mL; **3** precipitated as a dark purple crystalline powder (0.053 g, 0.078 mmol, 64%). After filtration and further reduction of the volume to 5 mL, the clear blue solution was set to crystallize using evaporation, $Et_2O$ layer, and $Et_2O$ diffusion techniques. In each case, large dark purple-black crystals of **3** (0.0215 g, 0.032 mmol, 26 %) were formed overnight. Both crystals and powder rapidly changed color upon exposure to air, becoming a royal blue hydroxo compound with the composition $C_{14}H_{34}Cl_2Cu_2N_4O_{12}$. IR (hydroxo compound, KBr disk, $cm^{-1}$): 3508 s, 3308 s, 3260 m, 2934 m, 2825 w, 1589 m, 1464 w, 1366 w, 1120 s, 1099 s, 1075 s, 899 w, 702 w, 622 m, 466 w. Elemental analysis for $C_{14}H_{34}Cl_2Cu_2N_4O_{12}$, actual (expected): C, 25.51 (25.93); H, 5.27 (5.29); N, 8.23 (8.64).

**Preparation of [{Cu(DAHC)(OH)}$_4$]($ClO_4$)$_4$·2.5MeOH (4).** A solution of $Cu(ClO_4)_2 \cdot 6H_2O$ (0.050 g, 0.135 mmol) in water (0.5 mL) was added to DAHC (0.025 g, 0.192 mmol) dissolved in methanol (10 mL). A color change to dark purple was observed, before the addition of 1 mL of water resulted in a color change to royal blue. After the mixture was stirred at room temperature for around 2 h, small royal blue crystals of **4** (0.0092 g, 0.007 mmol, 21%) were isolated in approximately 24 h by diffusion of diethyl ether into the methanolic solution. IR (KBr disk, $cm^{-1}$): 3411 s, 3225 s, 3168 s, 3112 s, 2925 m, 2890 m, 2850 w, 1602 s, 1457 m, 1403 m, 1366 m, 1343 w, 1258 w, 1147 s, 1088s, 1057s, 1068 s, 913 m, 714 m, 627 s, 466 m, 404 w. Elemental analysis for $C_{24}H_{60}Cl_4Cu_4N_8O_{24}$ (**4**, methanol removed by drying), actual (expected): C, 23.40 (23.23); H, 4.80 (4.87); N, 8.83 (9.03).

**Preparation of [{Cu(DAMC)(OH)}$_4$]($ClO_4$)$_4$·$H_2O$ (5).** A solution of $Cu(ClO_4)_2 \cdot 6H_2O$ (0.0920 g, 0.124 mmol) in water (0.5 mL) was added to DAMC (0.050 g, 0.173 mmol) dissolved in methanol (10 mL). A color change to dark purple was observed, before the addition of 1 mL of water resulted in a color change to royal blue. After the mixture was stirred at room temperature for around 4 h, the solution was filtered and concentrated in vacuo to a volume of ca. 5 mL. Small navy blue crystals of compound **5** (0.024 g, 0.018 mmol, 29%) were isolated in about 24 h by diffusion of diethyl ether into the methanolic solution. IR (KBr disk, $cm^{-1}$): 3508 s, 3308 s, 3260 m, 2934 m, 2825 w, 1589 m, 1464 w, 1366 w, 1120 s, 1099 s, 1075 s, 899 w, 702 w, 622 m, 466 w. Elemental analysis for $C_{28}H_{70}Cl_4Cu_4N_8O_{25}$ (5·$H_2O$), actual (expected): C, 25.58 (25.58); H, 5.25 (5.37); N, 8.36 (8.52).

**Preparation of [{$Cu_2(OH)_2$(GADACE)}$_2$]$Cl_4$·2MeOH·6$H_2O$ (6).** A methanolic solution of (1.32 mL) GADACE (0.025 g, 0.070 mmol) was added to a solution of $CuCl_2$ (0.0132 g, 0.098 mmol) in methanol (1 mL). The copper(II) chloride solution changed color rapidly from yellow-green to royal blue and became cloudy; sufficient water was added to make the cloudiness disappear. The solution was filtered after being stirred for 2 h and set to crystallize by ether diffusion. After 48 h, a blue solid was observed at the bottom of the crystallization tubes, and after around 7 days, a few royal blue crystals of **6** appeared on the side of the tube. Material recovered from the bottom of the tubes (0.016 g, 0.012 mmol, 55%) matched the infrared spectrum of the crystals and gave an elemental analysis result reasonably close to the calculated values for **6**. IR (KBr disk, $cm^{-1}$): 3437 s, 3253 w, 3117 w, 2925 m, 1719 s, 1596 m, 1458 w, 1365 w, 1153 m, 1022 m, 918 w, 783 w. Elemental analysis for $C_{34}H_{68}Cu_4Cl_4N_8O_{12}$, all crystal solvent removed under vacuum, actual (expected) C, 35.32 (34.70); H, 6.15 (5.82); N, 9.28 (9.51).

**Single-Crystal Structure Determination.** Suitable single crystals of **1**−**7** were mounted on the end of a thin glass fiber using Fomblin oil. X-ray diffraction intensity data were measured at 150 K on a Nonius Kappa-CCD diffractometer ($\lambda$(Mo K$\alpha$) = 0.7107 Å). Structure solution and refinement for **1**−**7** were carried out with SHELXS-97[31] and SHELXL-97[32] via WinGX.[33] Corrections for incident and diffracted beam absorption effects were applied using empirical[34] or numerical methods.[35] Compound **1** crystallized in the space group $P\bar{1}$, compounds **2**, **5**, and **6** in $C2/c$, compounds **3** and **7** in $P2_1/c$, and compound **4** in $P2_1/n$, as determined by systematic absences in the intensity data, intensity statistics, and the successful solution and refinement of the structures. All structures were solved by a combination of direct methods and difference Fourier syntheses and refined against $F^2$ by the full-matrix least-squares technique. Crystal data, data collection parameters, and refinement statistics for **1**−**7** are listed in Table 4.

## Results and Discussion

**Ligand/Complex Design Overview.** This study utilizes ligands that are based on a rigid 1,3,5-functionalized cyclohexane backbone containing a *cis*-1,3-diamino moiety. Our previous studies showed that when the trans moiety is an amino group, as for the ligand *cis*,*trans*-1,3,5-triaminocyclohexane (*trans*-TACH), a great deal of versatility can result because the *cis* chelator can be used to coordinate to a metal ion and the *trans* group can be protonated and anchor the unit in a hydrogen-bonded network.[36] By changing the *trans* group to hydroxy, then methoxy, and finally by linking two *cis*-1,3-diamino-cyclohexanes via a 5-carbon glutaryl group, we are able to explore the effects of altering the hydrogen-bond donor/acceptor properties of the ligand and also increase its preorganization (Figure 1).

**Monomer.** The smallest building block in this study, the mononuclear complex *anti*-[Cu(DAHC)$_2$]($ClO_4$)$_2$ (**1**), was isolated along with the copper methoxo dimer, [{Cu(DAHC)(OMe)}$_2$]($ClO_4$)$_2$·MeOH, **2**, by adding a small amount of aqueous sodium perchlorate in conditions which otherwise led to exclusive crystallization of the dimer (see Figure 2).

(31) Sheldrick, G. M. *Acta Crystallogr.* **1998**, *A46*, 467.
(32) *Programs for Crystal Structure Analysis*, release 97-2; Institut für Anorganische Chemie der Universität Göttingen: Göttingen, Germany, 1998.
(33) Farrugia, L. J. *J. Appl. Crystallogr.* **1999**, *32*, 837.
(34) Blessing, R. H. *Acta Crystallogr.* **1995**, *A51*, 33.
(35) Coppens, P.; Leiserowitz, L.; Rabinovich, D. *Acta Crystallogr.* **1965**, *A18*, 1035.
(36) Seeber, G.; Kögerler, P.; Kariuki, B. M.; Cronin, L. *Chem. Commun.* **2004**, 1580.

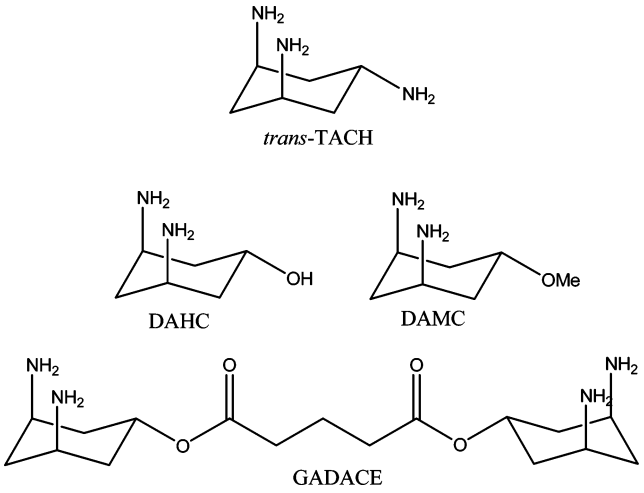


**Figure 1.** *trans*-TACH (top), DAHC, DAMC (middle), and GADACE (bottom) shown in their ring-flipped chelating conformations.

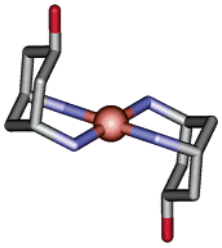

**Figure 2.** Representation of the complex cation *anti*-$[Cu(DAHC)_2]^{2+}$ in **1**: C, gray; O, red; N, purple; Cu, copper; H, omitted.

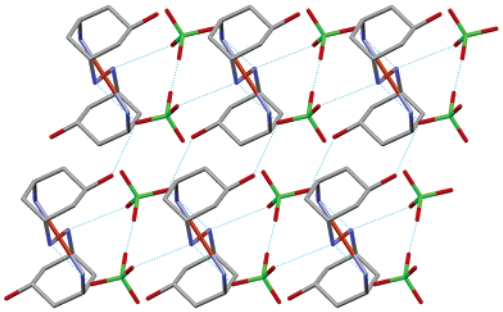

**Figure 3.** Hydrogen-bonded layer in *anti*-$[Cu(DAHC)_2](ClO_4)_2$ (**1**), viewed along the crystallographic *c* axis: C, gray; O, red; N, blue; Cl, green; Cu, copper; H, omitted. Hydrogen bonds are shown as bright blue dotted lines between the donor/acceptor positions.

It is thought that the increased ionic strength resulting from the addition of $NaClO_4$ encourages rapid crystallization of doubly charged compound **1**, which is likely to be the first species formed in the complexation reaction. In the absence of $NaClO_4$, this is able to remain in solution and equilibrates forming **2**.

The complex cation of **1** is identical to that previously reported in the copper fluoride complex *anti*-$[Cu(DAHC)_2]F_2 \cdot 2H_2O$.[17] Around the copper(II) center the square planar coordination geometry is close to the $C_{4v}$ ideal, with Cu−N bond lengths of 2.0221(15) and 2.0337(16) Å and N−Cu−N angles of 91.42(6) and 88.58(6)°. In contrast to the fluoride complex, no water molecules are included in the crystal lattice because of the limited hydrogen bonding properties of the perchlorate counterions (Figure 3). The cations form layers connected by hydrogen bonds that run parallel to the crystallographic *ab* plane, where hydrogen bonds extend from the ligand alcohol and amine donor groups to the perchlorate oxygens. As a consequence of the absence of included solvent, this compound does not undergo the solvent-driven geometry reorganization reported for its fluoride analogue.[17]

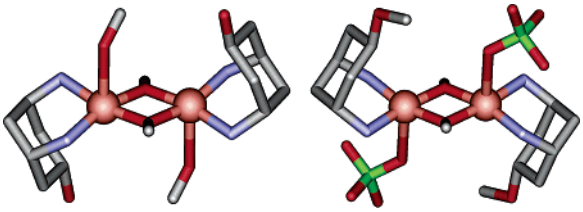

**Figure 4.** Dimers of the complex cation in $[\{Cu(DAHC)(OMe)\}_2](ClO_4)_2 \cdot MeOH$ (**2**, left) and $[\{Cu(DAMC)(OMe)(ClO_4)\}_2]$ (**3**, right). Color codes as in Figure 3.

**Table 1.** Summary of Distances, Angles, and Trigonality Indices ($\tau$) for Complexes **2** and **3**

| | bond distances (Å) | | | metal···metal distances (Å) | angles (deg)/ trigonality indices | |
|---|---|---|---|---|---|---|
| | Cu−O (apl) | Cu−O (bsl) | Cu−N (bsl) | Cu···Cu | $\tau$ | $\Phi_{Cu-O-Cu}$ |
| **2** | 2.479(7) | 1.929(3) | 2.001(4) | 3.0241(13) | 0.08 | 103.21(14) |
| **3** | 2.535(2) | 1.933(19) | 1.999(2) | 2.9993(7) | 0.12 | 101.77(9) |

**$Cu_2O_2$ Dimers.** Complexation of DAHC and DAMC with copper(II) perchlorate in methanol, without addition of sodium perchlorate, resulted in exclusive formation of the copper methoxo dimers $[\{Cu(DAHC)(OMe)\}_2](ClO_4)_2 \cdot MeOH$ (**2**) and $[\{Cu(DAMC)(OMe)(ClO_4)\}_2]$ (**3**) in moderate to high yields (Figure 4). Upon exposure to atmospheric moisture, both **2** and **3** quickly change color from a dark purple to royal blue, lose crystallinity, and rearrange to form copper−hydroxo structures which are believed to be the $Cu_4O_4$ cubanes **4** and **5**. This occurs so rapidly that an infrared spectrum of **2** required the use of a diamond anvil setup with the material kept in a drop of mother liquor; as soon as this evaporated the color and spectrum would change. Elemental analysis, infrared spectra, and magnetic measurements on the isolated dry compounds were all identical to the cubanes **4** and **5**.

In these compounds, the copper(II) centers are bridged by two $\mu_2$-methoxo ligands to form a planar rhombic $Cu_2O_2$ dimer, with the remaining basal coordination sites on the square pyramidal copper centers occupied by the chelating amine ligands which are arranged anti to each other (Figure 4). Apical coordination is provided by solvent or counterions, again arranged anti to each other, at a considerably elongated Cu−O distance (Table 1). In compound **2**, this site is occupied by a disordered methanol molecule shared with the copper of another dimer, whereas in **3**, it is filled by a perchlorate counterion. Furthermore, in **3** the apical coordination distance is substantially longer, while a tighter Cu−O−Cu angle results in a shorter Cu···Cu separation. Both complexes show a certain amount of distortion from the ideal square pyramidal geometry with trigonality indices, $\tau$, of 0.08 and 0.12, respectively.[37]

(37) Addison, A. W.; Rao, T. N.; Reedijk, J.; Van Rijn, J.; Verschoor, G. C. *J. Chem. Soc., Dalton Trans.* **1984**, 1349.

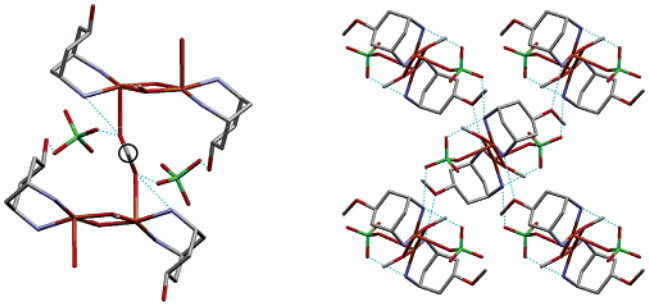

**Figure 5.** (left) Association of two $[\{Cu(DAHC)(OMe)\}_2]^{2+}$ cations in the chains of **2** (the carbon of the disordered methanol ligand is circled in black). (right) A section of the hydrogen-bonded layer of **3** viewed along the crystallographic *a* axis. Color codes as in Figure 3.

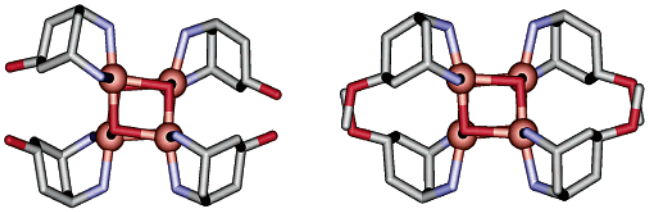

**Figure 6.** Structure of the complex cations in $[\{Cu(OH)(DAHC)\}_4](ClO_4)_4$ (**4**, left) and $[\{Cu(OH)(DAMC)\}_4](ClO_4)_4$ (**5**, right). Color codes as in Figure 3.

As expected, methylation of the ligand alcohol group results in a number of differences between the extended structures, most significantly inclusion of disordered solvent molecules in **2** which appear to provide a linkage via coordinate bonds between the complex cations. Furthermore, while **2** consists of chains of cations linked by these disordered methanol molecules and hydrogen bonds, **3** is built up of hydrogen-bonded layers (Figure 5). These differences may be explained by the presence of ligand alcohol groups which act as hydrogen-bond donors in compound **2**; hydrogen bonds from these donors to the perchlorate counterions (donor−acceptor distance = 2.873 Å) prevent their coordination to the copper centers in this structure, so that the apical copper coordination sites instead form weak interactions with the solvent. However, in **3** the perchlorate counterion coordinates to the dimer unit, subtly changing its shape and altering its packing in the crystal lattice.

**$Cu_4O_4$ Cubanes.** Further small changes to the reaction conditions led to aggregation of the dimer units into the cubane structures $[\{Cu(OH)(DAHC)\}_4](ClO_4)_4$ (**4**) and $[\{Cu(OH)(DAMC)\}_4](ClO_4)_4$ (**5**), with the bridging ligands changed to hydroxo groups (Figure 6). Interestingly, hydroxo-bridged cubanes are far rarer than their alkoxo-bridged counterparts, with only 3 of 69 structurally characterized $Cu_4O_4$ cubane motifs having hydroxo bridges.[38] Furthermore, compound **5** indicates that the dimers rearrange to their cubane analogues upon exposure to water (atmospheric moisture), since it retains its crystallinity when kept in air for many months. Specifically, compound **3** transforms to compound **5** upon exposure to moisture.

(38) A search of the Cambridge Structural Database (version 5.26, November 2004) revealed that out of 69 deposited $Cu_4O_4$ cubane motifs, only 3 were hydroxo bridged. A far larger number (124) of $Cu_2(OH)_2$ dimers were found.

**Table 2.** Cu···Cu Distances (Å) and Cu−O−Cu Angles (deg) in the Cubanes $[\{Cu(OH)(DAHC)\}_4](ClO_4)_4$ (**4**) and $[\{Cu(OH)(DAMC)\}_4](ClO_4)_4$ (**5**)

| | **4** | | **5** | |
|---|---|---|---|---|
| type of face | $R_{Cu\cdots Cu}$ | $\Phi_{Cu-O-Cu}$ | $R_{Cu\cdots Cu}$ | $\Phi_{Cu-O-Cu}$ |
| intradimer | 3.031(1) | 100.42(16) | 3.035(2) | 99.4(3) |
| | | 99.78(16) | | 100.5(3) |
| intradimer | 3.035(1) | 100.64(17) | 3.035(2) | 99.4(3) |
| | | 99.91(16) | | 100.5(3) |
| interdimer | 3.278(1) | 100.27(16) | 3.213(2) | 95.9(3) |
| | | 98.61(15) | | 96.4(3) |
| interdimer | 3.192(1) | 96.25(15) | 3.213(2) | 95.9(3) |
| | | 95.99(15) | | 96.4(3) |
| interdimer | 3.224(1) | 97.13(16) | 3.259(2) | 97.4(3) |
| | | 98.55(15) | | 97.4(3) |
| interdimer | 3.220(1) | 98.19(15) | 3.239(2) | 97.4(3) |
| | | 96.41(15) | | 97.4(3) |

Cubane synthesis was best achieved by adding around 13 vol % water to the reaction mixture. While it is clear that addition of water to these methanolic solutions favors hydroxo-bridged structures because of its lower $pK_a$,[39] this alone does not explain the formation of cubanes rather than dimers, given that hydroxo-bridged dimers are far more common than cubanes.[38] Consequently, it is postulated that higher concentrations of water help prevent the weak apical coordination of anions or solvent through competing hydrogen bonding interactions.[17,40] Without these ligands blocking the apical coordination sites, the association of dimers into cubanes becomes possible.

The $Cu_4O_4$ core of these structures has four $\mu_3$-hydroxo bridges situated at alternate vertexes to four 5-coordinate copper(II) centers and can be divided into two $Cu_2O_2$ dimers: the intradimer Cu−O bond lengths (1.964(4)−1.997(6) Å) are considerably shorter than the equivalent interdimer distances (2.268(4)−2.328(4) Å). Around the Jahn−Teller-distorted square pyramidal Cu(II) ions ($\tau$ ranges from 0.04 to 0.17 in **4** and 0.08 to 0.09 in **5**) two of the basal coordination sites are taken by the amines of a chelating DAHC or DAMC ligand, with the remainder occupied by $\mu_3$-hydroxo bridges. Note that in both structures the ligands are arranged syn across each dimer subunit, in contrast to the anti orientation observed in the isolated copper methoxo dimers **2** and **3**. Presumably, anti orientation of the ligands would obstruct aggregation to form the tetramer.

Despite their overall similarity, the two structures differ in terms of their coordination geometry and crystal packing. Notably, the DAHC cubane, **4**, is substantially less regular than the DAMC analogue, **5**. This asymmetry is reflected in the fact that all six faces of the cube have a different geometry as indicated by the Cu···Cu distances and Cu−O−Cu angles in Table 2. By contrast, the asymmetric unit of the more regular DAMC cubane, **5**, consists of only a $Cu_2O_2$ dimer with two perchlorate counterions, allowing it to be considered as two identical but asymmetric dimers connected by Cu−O bonds. Consequently, this cubane has four, rather than six, different face geometries (Table 2).

As expected, variation of the *trans*-positioned "tail" group (methoxy or hydroxyl) also results in differences in the

(39) *CRC Handbook of Chemistry and Physics*, 81st ed.; CRC Press: New York, **2000**.
(40) Carlucci, L.; Ciani, G.; Proserpio, D. *Chem. Commun.* **2004,** 380.

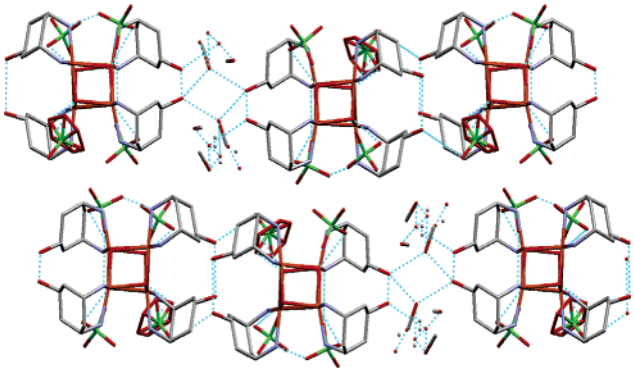

**Figure 7.** Hydrogen-bonded layers in **4** viewed along the crystallographic *a* axis (the layers are situated parallel to the *ab* plane). The picture is complicated by disorder in the counterions and solvent molecules. Color codes as in Figure 3.

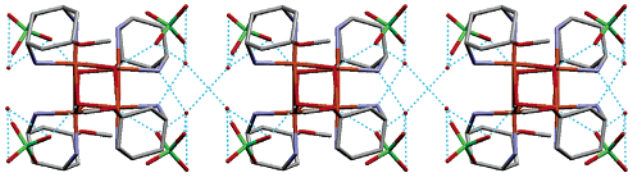

**Figure 8.** Hydrogen-bonded chain in **5** viewed along the crystallographic *a* axis. Color codes as in Figure 3.

extended structures, which may to some extent cause the differences between the two complex cations. Contrary to the dimers, in the case of the cubanes, the crystals formed with DAHC (**4**) show a higher dimensionality hydrogen-bonded network (see Figure 7). The $[\{Cu(OH)(DAHC)\}_4]^{4+}$ complex cations are packed in hydrogen-bonded layers running parallel to the crystallographic *ab* plane, with hydrogen bonds mediated by counterions and methanol molecules (Figure 6). In **5** however, $[\{Cu(OH)(DAMC)\}_4]^{4+}$ complex cations and water molecules are packed in a one-dimensional hydrogen-bonded array running parallel to the crystallographic *b* axis (Figure 8). Note that, in contrast to the OH tail group in **4**, the methoxy tail group in this structure neither accepts nor donates hydrogen bonds, reducing the amount of interaction between the complex and the network. This may explain the more symmetrical cubane core of **5**: fewer interactions with the hydrogen-bonded network should reduce distortions in the complex.

**Magnetic Properties.** The magnetic susceptibility data of **4** and **5** (corrected for diamagnetic contributions) are shown in Figure 9 and, once rescaled to account for their greater molecular mass, are identical to the data obtained for **2** and **3** because of the rapid condensation of these dimers to cubanes (see above). Despite the similarity of the magnetically relevant $Cu_4O_4$ core structures in **4** and **5**, the susceptibility curves are vastly different with **5** displaying stronger antiferromagnetic coupling than **4**, which immediately illustrates the well-known sensitivity of the oxo-mediated $Cu^{II}-Cu^{II}$ exchange on the exact Cu−O distances and the Cu−O−Cu bond angle.[23−28] In both cases, strong overall antiferromagnetic exchange is observed, and even at room temperature, $\chi T$ is significantly below the expected spin-only value of 1.73 emu K mol$^{-1}$ for four uncorrelated, Jahn−Teller-distorted $s = 1/2$ $Cu^{II}$ centers (assuming an isotropic *g* factor of $g_{iso} = 2.15$). We found that for **5** a fit to an isotropic Heisenberg model we had to break up the six exchange interactions per $Cu_4O_4$ cluster into four exchange constants, $J_1-J_4$ (Figure 10), matching the four different $Cu_2O_2$ face geometries of the $Cu_4O_4$ cubane core (see above). This results in the following spin Hamiltonian:

$$\boldsymbol{H} = J_1(\mathbf{S}_1\mathbf{S}_2 + \mathbf{S}_3\,\mathbf{S}_4) + J_2(\mathbf{S}_1\mathbf{S}_4 + \mathbf{S}_2\mathbf{S}_3) + J_3\mathbf{S}_1\mathbf{S}_3 + J_4\mathbf{S}_2\mathbf{S}_4$$

Here, the pair of oppositely arranged, strongly antiferromagnetic interactions $J_1$ between Cu1−Cu2 and Cu3−Cu4 correspond to the intradimer exchange of the condensed dimer halves ($J_1 = -217.0$ K for **5**). To achieve a reasonable fit, weak and strong ferromagnetic exchange interactions between those halves have to be used for $J_2$, $J_3$, and $J_4$. For the DAMC derivative **5**, the weaker ferromagnetic exchanges ($J_3 = 8.5$ K, $J_4 = 37.0$ K) can be rationalized by the presence of two faces of the $Cu_4O_4$ cube with two Cu−O−Cu angles

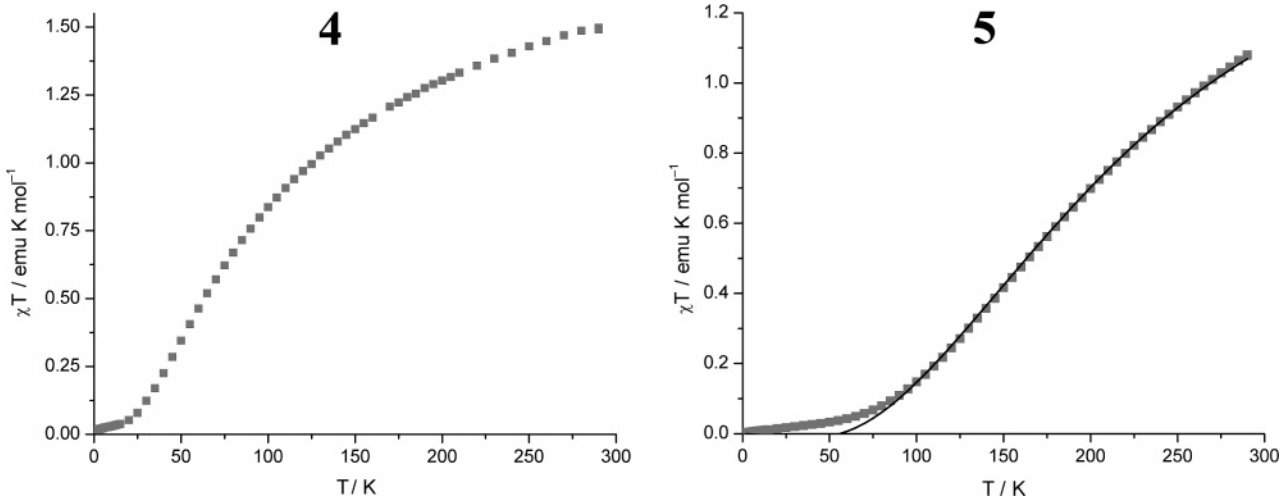


**Figure 9.** Temperature dependence of $\chi T$ for **4** (left) and **5** (right) at 0.1 T. Experimental data (corrected for diamagnetic contributions $\chi_{dia}(\mathbf{4}) = -6.16 \times 10^{-4}$ emu mol$^{-1}$ and $\chi_{dia}(\mathbf{5}) = -6.20 \times 10^{-4}$ emu mol$^{-1}$) are represented as gray squares, and the best fit for **5** for the Heisenberg models used(see text) is shown as a black curve. Differences at higher magnetic fields (up to 5.0 T) are minimal and indicate a presence of less than 0.005 detached $Cu^{II}$ centers per formula unit that contribute to a minimal paramagnetic background. Neither **4** nor **5** display Curie−Weiss behavior.

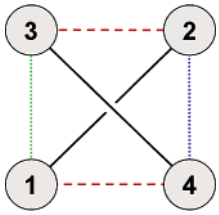


**Figure 10.** Scheme of the magnetic exchange interactions used in the Heisenberg models for both **4** and **5**. The numbered spheres denote the four $Cu^{II}$ centers, the lines represent the four different types of intracubane exchange ($J_1$, black lines; $J_2$, dashed red lines; $J_3$, dotted green line; $J_4$, dotted blue line). Note that the Cu−Cu interactions, Cu1−Cu2 and Cu3−Cu4, characterized by $J_1$, correspond to the hypothetical intradimer interactions.

**Table 3.** Cu···Cu Distances (Å) and Cu−O−Cu Angles (deg) in $[\{Cu_2(OH)_2(GADACE)\}_2]Cl_4 \cdot 2MeOH \cdot 6H_2O$ (**6**)

| type of face | $R_{Cu\cdots Cu}$ | $\Phi_{Cu-O-Cu}$ |
|---|---|---|
| intradimer | 3.0305(5) | 99.88(9), 101.12(9) |
| intradimer | 3.0305(5) | 99.88(9), 101.12(9) |
| interdimer | 3.2283(5) | 96.04(8), 96.04(8) |
| interdimer | 3.2298(5) | 95.29(8), 96.44(8) |
| interdimer | 3.2298(5) | 95.29(8), 96.44(8) |
| interdimer | 3.2916(5) | 97.89(8), 97.89(8) |

of 97.4(3)° (which are close to 97.5°, the empirical threshold value for antiferromagnetic coupling in oxo-bridged $Cu_2$ dimers) and with longer Cu···Cu distances (3.239(2)/3.259(2) Å, see Table 2). The stronger ferromagnetic coupling pair ($J_2$ = 309.8 K) is provided by another two faces with shorter Cu···Cu separations (3.213(2) Å) and smaller Cu−O−Cu angles (96.4(3)° and 95.9 (3)°).

For the less symmetric DAHC derivative **4**, a spin Hamiltonian would need to employ six exchange energies, $J_1-J_6$, to accommodate the different Cu−O−Cu geometries. However, as the temperature dependence of the susceptibility is the only data to which such a model can be fitted, isospectrality (i.e., several different sets of $J_1-J_6$ resulting in the same or virtually the same thermodynamic properties) prevents an unambiguous assignment of these exchange energies. Future work on a full quantitative analysis of the magnetic properties of **4** therefore requires additional experimental data (e.g., derived from the field dependence of the low-temperature (mK) magnetization or inelastic neutron scattering).

**Facially Bridged Cubane: Complexation of GADACE with Copper(II) Chloride.** Replacement of the DAHC or DAMC monochelator with GADACE, a ligand in which two DAHC groups are linked by esterification with the dicarboxylic glutaric acid, and complexation with copper(II) chloride also resulted in cubane formation. The formation of the cubane structure **6**, rather than a dimer, is the result of the large amounts of water (around 20 vol %) added to dissolve the precipitate which formed upon addition of the metal salt to the reaction solution. Furthermore, the GADACE ligand may help direct cubane formation, by ensuring that the two DAHC cores of each dimer project in the same direction leaving one face unobstructed to allow aggregation, by simultaneously blocking the other face from coordination

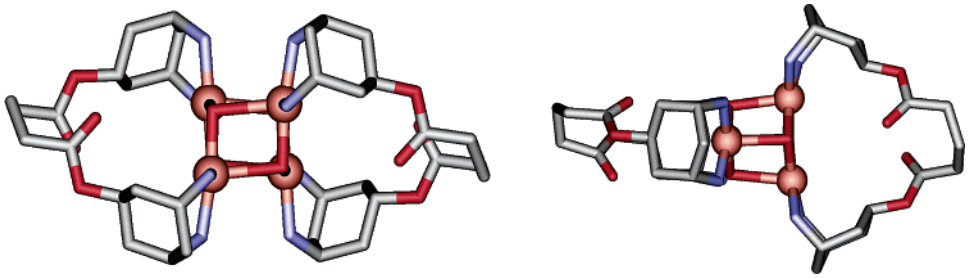

**Figure 11.** Views of the complex cation in $[\{Cu_2(OH)_2(GADACE)\}_2]Cl_4 \cdot 2MeOH \cdot 6H_2O$ (**6**) chosen to best show the linking $C_5$ unit connecting each of the diamino cores. Color codes as in Figure 3.

**Table 4.** Crystallographic Data for **1**−**7**[a]

| | **1** | **2** | **3** | **4** | **5** | **6** | **7** |
|---|---|---|---|---|---|---|---|
| empirical formula | $C_{12}H_{28}Cl_2CuN_4O_{10}$ | $C_{15}H_{38}Cl_2Cu_2N_4O_{13}$ | $C_{16}H_{38}Cl_2Cu_2N_4O_{12}$ | $C_{26.5}H_{70}Cl_4Cu_4N_8O_{26.5}$ | $C_{28}H_{70}Cl_4Cu_4N_8O_{25}$ | $C_{36}H_{88}Cl_4Cu_4N_8O_{20}$ | $C_7H_{14}CuN_2O_4$ |
| Fw. (g mol$^{-1}$) | 522.82 | 680.47 | 676.48 | 1320.87 | 1314.88 | 1349.10 | 253.74 |
| cryst syst | triclinic | monoclinic | monoclinic | monoclinic | monoclinic | monoclinic | monoclinic |
| $a$ (Å) | 6.9536(2) | 23.3788(7) | 11.3227(3) | 10.6310(2) | 24.1690(9) | 24.1409(11) | 10.1040(5) |
| $b$ (Å) | 8.1129(3) | 8.5014(3) | 10.1481(5) | 25.6433(4) | 10.7545(3) | 15.4935(8) | 6.8627(3) |
| $c$ (Å) | 9.6905(3) | 13.5422(4) | 12.3980(6) | 19.6386(4) | 20.1015(8) | 15.5757(5) | 13.8514(8) |
| α (deg) | 105.394(2) | 90 | 90 | 90 | 90 | 90 | 90 |
| $\beta$ (deg) | 108.615(2) | 105.303(2) | 110.665(3) | 102.003(1) | 111.001(2) | 105.515(3) | 94.673(2) |
| $\gamma$ (deg) | 99.232(2) | 90 | 90 | 90 | 90 | 90 | 90 |
| space group | $P\bar{1}$ | $C2/c$ | $P_{21}/c$ | $P_{21}/n$ | $C2/c$ | $C2/c$ | $P2_1/c$ |
| $V$ (Å$^3$) | 481.17(3) | 2596.11(14) | 1332.92(10) | 5236.71(17) | 4877.8(3) | 5613.4(4) | 957.27(8) |
| $Z$ | 1 | 4 | 2 | 4 | 4 | 4 | 4 |
| $\rho_{calcd}$ (g cm$^{-1}$) | 1.804 | 1.741 | 1.686 | 1.675 | 1.790 | 1.596 | 1.761 |
| $\mu$ (mm$^{-1}$) | 1.474 | 1.913 | 1.859 | 1.894 | 2.031 | 1.761 | 2.272 |
| $T$ (K) | 150(2) | 150(2) | 150(2) | 150(2) | 150(2) | 150(2) | 150(2) |
| no. observations (unique) | 6802 (1878) | 18 051 (2558) | 16 425 (2619) | 62 023 (10 017) | 19 061 (4186) | 27 050 (4579) | 9131 (1878) |
| residuals: $R$, $R_w$ | 0.0245 0.0598 | 0.0563 0.1411 | 0.0363 0.0728 | 0.0621 0.1239 | 0.0833 0.1917 | 0.034 0.081 | 0.0347 0.0913 |

[a] $R = \Sigma||F_o| - |F_c||/\Sigma|F_o|$. $R_w = \{\Sigma[w(F_o^2 - F_c^2)^2]/\Sigma[w(F_o^2)^2]\}^{1/2}$.

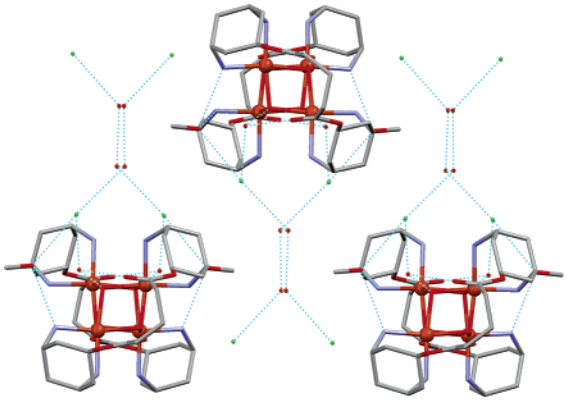

**Figure 12.** Packing of hydrogen-bonded subunits parallel to the crystallographic *c* axis (viewed from the *a* axis) in $[\{Cu_2(OH)_2(GADACE)\}_2]Cl_4 \cdot 2MeOH \cdot 6H_2O$, **6**. Color codes as in Figure 3.

of solvent or counterions and providing structural support for two faces of the cube (Figure 11). This is reflected in the substantially higher yield (55%) obtained for this compound by comparison with the DAHC and DAMC structures (best value 29%).

The structure of **6** bears more resemblance to the DAMC cubane **5** than its DAHC analogue, **4**, the asymmetric unit demonstrating that it is constructed from two identical but asymmetric $Cu_2O_2$ dimers connected by Cu−O bonds. As observed in both of the other cubanes, the structure can be divided into two dimers with short Cu−O bonds (1.964(2)−1.9859(6) Å), linked by longer Cu−O bonds (2.345(2)−2.389(4) Å) between the dimers. The distortion from ideal square pyramidal geometry at the copper centers is slightly lower than that observed in the other cubanes, with $\tau = 0.04$ and 0.08 at the two crystallographically independent coppers.

Like **5**, the complex cation shows four different values for the six Cu···Cu separations, and the distribution of the bond angles indicates that there are consequently four different geometries for the six faces of the cube (Table 3). However, the intradimer Cu···Cu distances are shorter than in **5**, and the corresponding Cu−O−Cu angles slightly wider. The interdimer Cu···Cu distances are longer, and the Cu−O−Cu angles are tighter. Although magnetic data were not collected for **6**, broadly similar behavior to **5** is expected but with both the ferromagnetic and antiferromagnetic interactions likely to be stronger.[23,27]

Large amounts of solvent are included in the crystal structure, resulting in an intriguing zero-dimensional hydrogen-bonded network which does *not* connect the complex cations in the solid state (Figure 12). Instead, a series of independent, "miniature" hydrogen-bonded networks pack in interpenetrating lines parallel to the crystallographic *c* axis. Each "mini-network" contains the $[\{Cu_2(OH)_2(GADACE)\}_2]^{4+}$ cation, four chloride counterions, two methanols, and four water molecules. Two methanol molecules and two waters hydrogen bond with each cation via the amines, hydroxo ligands, and carbonyl group, and, in turn, donate hydrogen bonds to two chloride ions each connected to one corner of a water tetramer. The network is completed by another two chloride ions at the remaining corners of the water tetramer. Just as in **5**, the lower dimensionality of the hydrogen-bonded network may correlate with the more highly symmetric nature of the cubane.

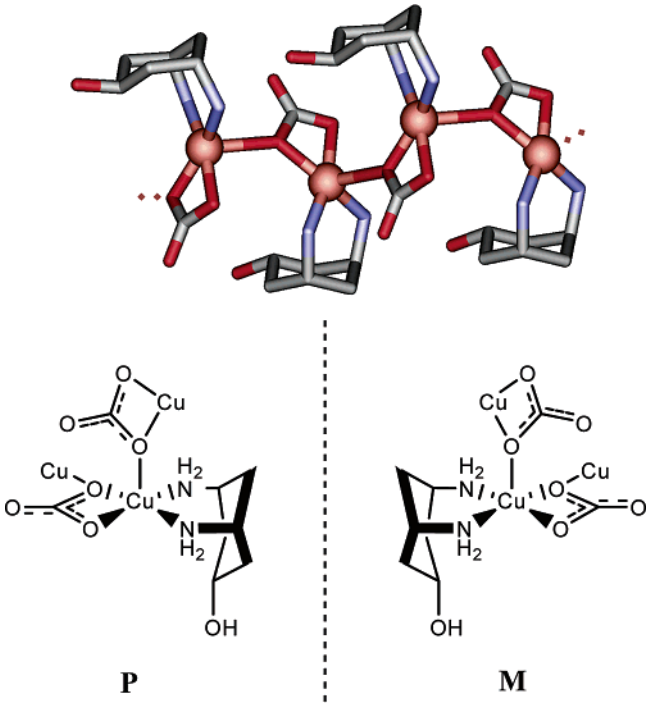


**Figure 13.** The $[\{Cu(DAHC)(CO_3)\}_n]$ polymer, **7**: (top) assembly of $[Cu(DAHC)(CO_3)]$ units into a chain and (bottom) the chiral copper(II) center in **7**.

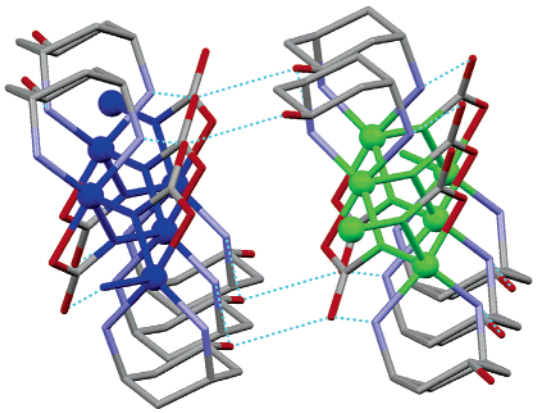

**Figure 14.** Association of the P- and M-enantiomers of $[Cu(DAHC)(CO_3)]_n$, **7**, to form a hydrogen-bonded layer. Cu and $\mu$-O are blue (P) or green (M); other color codes as in Figure 3.

**Polymeric Structure.** Also isolated in small quantities from the same reaction mixture as **1** were bright blue crystals of the carbonato-bridged coordination polymer $[\{Cu(DAHC)(CO_3)\}_n]$ (**7**), which forms in the presence of atmospheric carbon dioxide (Figure 13). The carbonato ligands chelate to one copper center, while one of the chelating oxygens acts as a $\mu_2$ bridge to the next copper in the chain. At the copper(II) centers, a distorted square pyramidal geometry ($\tau = 0.19$) is observed, with basal coordination provided by one chelating DAHC molecule and one chelating $\kappa_2$-carbonato ligand. The basal bond lengths average 1.967(2) Å to nitrogen and 1.984(2) and 1.993(2) Å to oxygen, with substantially weaker coordination implied by a longer apical Cu−O bond length of 2.445(2) Å.

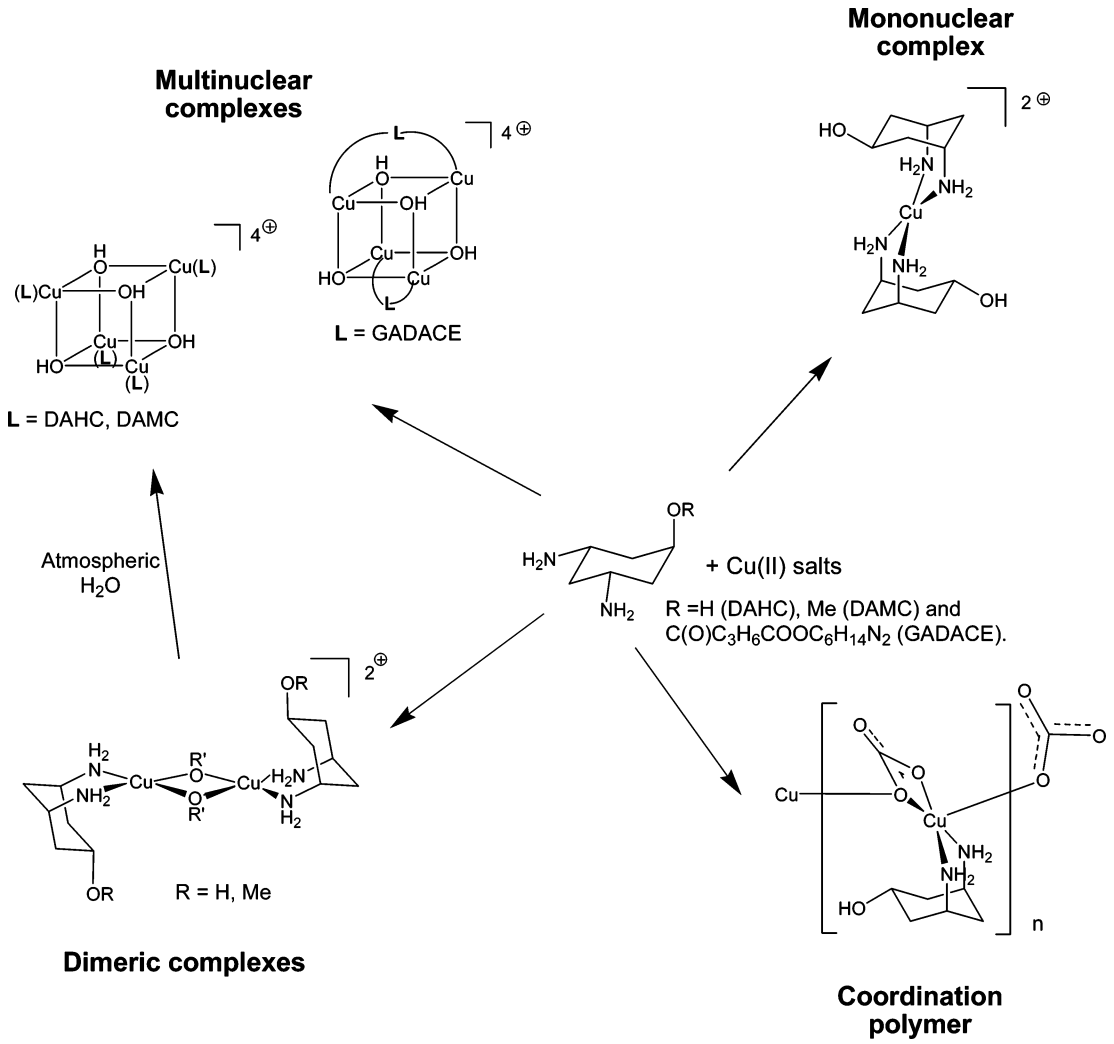


**Figure 15.** Summary of the coordination chemistry of the DAHC, DAMC, and GADACE ligands with $Cu^{II}$.

The extended crystal structure shows that the carbonato-bridged chains propagate as both left (anticlockwise, M-enantiomer) and right-handed (clockwise, P-enantiomer) helices parallel to the crystallographic *b* axis (Figures 13 and 14). The presence of both enantiomers within the same crystal is reflected in the centrosymmetric space group ($P2_1/c$), while the chirality within the chains occurs when [Cu(DAHC)($CO_3$)] monomers condense through the formation of bridges between acetate oxygens and vacant apical copper coordination sites.

Intramolecular hydrogen bonds donated by DAHC amine groups to carbonato oxygens and the oxygens of other DAHC ligands help stabilize the 1D coordination polymer, while the chains are linked by hydrogen bonds donated from the DAHC alcohol groups to the carbonato ligands of neighboring chains (Figure 14). This results in the connection of the coordination chains into hydrogen-bonded layers which extend parallel to the *bc* plane.

## Summary

One mononuclear complex, two new copper-alkoxo dimers, three new copper-hydroxo cubanes, and a carbonato-bridged infinite-chain coordination complex have been synthesized using the ligand DAHC and its derivatives DAMC and GADACE. With the smaller ligands, DAHC and DAMC, the type of resulting complex cation structure (monomer, dimer, cubane, or polymer) appears to be largely controlled by the solvent mixture and ionic strength employed, while varying the ligand causes subtle adjustments in the geometry of the coordination compounds (Figure 15). This solvent control is to be expected because of the similarity of the ligands, and it requires only relatively small changes in the solvent mixture to be effective, with the delicate balance being emphasized by the facile conversion of the copper-methoxo dimers to copper-hydroxo cubanes in the solid state. It can be explained by the involvement of secondary noncovalent interactions, most particularly hydrogen bonding, which compete with and influence coordinative bonding. For example, increasing the concentration of water encourages the formation of cubanes, rather than dimers, as coordinated counterions or solvent molecules which otherwise may block aggregation become "trapped" by hydrogen-bonding interactions with the added water. The nature of the counterion, in this case perchlorate, may be quite important to this behavior: since perchlorate coordinates only very weakly, hydrogen bonding can offer more effective competition than

it might for a more strongly coordinating anion. On the other hand, changing the ligand has more subtle, but potentially significant, effects. The use of DAHC, with an alcohol group, rather than DAMC, with a methoxy group, helps prevent coordination of the perchlorate anion in dimers as the alcohol is able to replace a coordinate bond to copper with a hydrogen bond. In cubanes, this results in a less symmetric structure as the hydrogen-bond donor provides a "handle" allowing the network to exert distorting forces on the complex cation. Changing the ligand also influences the dimensionality and construction of the hydrogen-bonded networks that build up the crystal. In the case of GADACE, the increased preorganization of the ligand has been shown to allow a more facile route to the formation of the cubane clusters producing correspondingly higher yields.

## Conclusions

The three cubanes and two dimers presented demonstrate the possibilities of ligand design, combined with variation of reaction conditions, for the control of structure in the complex cations of multinuclear coordination compounds. Furthermore, such an approach may allow fine-tuning of coordination bond angles and adjustment of interactions between complex cations in the solid state, in a way which is likely to influence the magnetic and reactive properties of the compounds. It is clear from this study that, with the smaller ligands, the solvent system and reaction conditions used have a more significant impact in controlling complex shape than the ligand, while their dinucleating analogues have stronger directing effects, a common observation in coordination chemistry. However, it is also clear that study of a number of related complexes, as detailed here, can allow a certain level of understanding of how secondary noncovalent interactions, here, hydrogen bonding, help direct the structure of multinuclear coordination compounds. In the context of our work, apparent directing effects are the competition between weak coordination of anions in the apical position and hydrogen bonding to these anions by water, in a way that can allow some control over complex nuclearity. Further studies of this nature may therefore promote a more rational approach in this field and will also involve developing the coordination chemistry of the GADACE ligand, which remains relatively unexplored. This ligand provides a particularly interesting opportunity since it may be able to influence the structure of the complex cation by taking different conformations. While the magnetic and catalytic properties of copper oxo dimers and cubanes are well-known, it is also anticipated that the extension of this approach to other, most particularly higher-spin, metal centers may produce interesting new materials.

**Acknowledgment.** J.F. would like to thank the EPSRC and D.L. would like to thank the Leverhulme Trust for funding. We thank Arkady Ellern (Department of Chemistry, Iowa State University) for valuable help with X-ray diffraction. Ames Laboratory is operated for the U.S. Department of Energy by Iowa State University under Contract No. W-7405-Eng-82.

**Supporting Information Available:** Crystallographic data in CIF format. This material is available free of charge via the Internet at http://pubs.acs.org.

IC051647T